2015-12

Silicon controlled switch for detection of ionizing radiation

Kjono, Karl J.

Monterey, California: Naval Postgraduate School

NAVAL POSTGRADUATE SCHOOL

MONTEREY, CALIFORNIA

THESIS

SILICON CONTROLLED SWITCH FOR DETECTION OF IONIZING RADIATION

by

Karl J. Kjono

December 2015

Thesis Advisor: Gamani Karunasiri
Co-Advisor: Fabio Alves

Approved for public release; distribution is unlimited

THIS PAGE INTENTIONALLY LEFT BLANK

REPORT DOCUMENTATION PAGE			Form Approved OMB No. 0704–0188
Public reporting burden for this collection of information is estimated to average 1 hour per response, including the time for reviewing instruction, searching existing data sources, gathering and maintaining the data needed, and completing and reviewing the collection of information. Send comments regarding this burden estimate or any other aspect of this collection of information, including suggestions for reducing this burden, to Washington headquarters Services, Directorate for Information Operations and Reports, 1215 Jefferson Davis Highway, Suite 1204, Arlington, VA 22202-4302, and to the Office of Management and Budget, Paperwork Reduction Project (0704-0188) Washington, DC 20503.			
1. AGENCY USE ONLY *(Leave blank)*	**2. REPORT DATE** December 2015	**3. REPORT TYPE AND DATES COVERED** Master's thesis	
4. TITLE AND SUBTITLE SILICON CONTROLLED SWITCH FOR DETECTION OF IONIZING RADIATION		**5. FUNDING NUMBERS**	
6. AUTHOR(S) Karl J. Kjono			
7. PERFORMING ORGANIZATION NAME(S) AND ADDRESS(ES) Naval Postgraduate School Monterey, CA 93943-5000		**8. PERFORMING ORGANIZATION REPORT NUMBER**	
9. SPONSORING /MONITORING AGENCY NAME(S) AND ADDRESS(ES) N/A		**10. SPONSORING / MONITORING AGENCY REPORT NUMBER**	
11. SUPPLEMENTARY NOTES The views expressed in this thesis are those of the author and do not reflect the official policy or position of the Department of Defense or the U.S. Government. IRB Protocol number ____N/A____.			
12a. DISTRIBUTION / AVAILABILITY STATEMENT Approved for public release; distribution is unlimited		**12b. DISTRIBUTION CODE**	

13. ABSTRACT (maximum 200 words)

The purpose of this thesis is to utilize the developed knowledge of key semiconductor components at the Naval Postgraduate School (NPS) and build a circuit design toward the specific goal of detecting CS-137 sources. A Silicon-Controlled Switch (SCS), under the presence of a direct current (DC) voltage bias (V_{BIAS}), was connected in series to a resistor and capacitor (RC) load. Additionally, a photodiode (PD) was connected to the anode gate (AG) of the SCS. The PD produced a triggering current that allowed the SCS-based circuit to create self-terminating pulses by operating in the SCS intermediate state. V_{BIAS} and PD produced current on the AG of the SCS where the methods for triggering self-terminating pulses. Various circuit elements such as a Zener (Zn) diode connected to the AG, feedback resistor (RF), and RC load were varied to achieve diverse pulsation results. The final circuit design produced a circuit that had ten times the resolution and five times the sensitivity of previous NPS silicon controlled rectifier (SCR) based circuits. Additionally, the circuit in this thesis was able to detect AM-241 and CS-137 sources for the first time at NPS. Future NPS thesis research is proposed to further understand and fine-tune semi-conductor–based radiation detectors. It is proposed that future naval feasibility assessments be centered on the signal amplification and processing techniques from SCS-based circuits.

14. SUBJECT TERMS Silicon-Controlled Switch, Pulse Generation Circuit, semiconductors, Solid-State Radiation Detectors, radiation detection, amplifier, signal processing			**15. NUMBER OF PAGES** 59
			16. PRICE CODE
17. SECURITY CLASSIFICATION OF REPORT Unclassified	**18. SECURITY CLASSIFICATION OF THIS PAGE** Unclassified	**19. SECURITY CLASSIFICATION OF ABSTRACT** Unclassified	**20. LIMITATION OF ABSTRACT** UU

NSN 7540–01-280-5500 Standard Form 298 (Rev. 2–89)
Prescribed by ANSI Std. 239–18

THIS PAGE INTENTIONALLY LEFT BLANK

Approved for public release; distribution is unlimited

SILICON CONTROLLED SWITCH FOR DETECTION OF IONIZING RADIATION

Karl J. Kjono
Lieutenant, United States Navy
B.S., United States Naval Academy, 2009

Submitted in partial fulfillment of the
requirements for the degree of

MASTER OF SCIENCE IN APPLIED PHYSICS

from the

NAVAL POSTGRADUATE SCHOOL
December 2015

Approved by: Gamani Karunasiri
Thesis Advisor

Fabio Alves
Co-Advisor

Kevin Smith
Chair, Department of Physics

THIS PAGE INTENTIONALLY LEFT BLANK

ABSTRACT

The purpose of this thesis is to utilize the developed knowledge of key semiconductor components at the Naval Postgraduate School (NPS) and build a circuit design toward the specific goal of detecting CS-137 sources. A Silicon-Controlled Switch (SCS), under the presence of a direct current (DC) voltage bias (V_{BIAS}), was connected in series to a resistor and capacitor (RC) load. Additionally, a photodiode (PD) was connected to the anode gate (AG) of the SCS. The PD produced a triggering current that allowed the SCS-based circuit to create self-terminating pulses by operating in the SCS intermediate state. V_{BIAS} and PD produced current on the AG of the SCS where the methods for triggering self-terminating pulses. Various circuit elements such as a Zener (Zn) diode connected to the AG, feedback resistor (RF), and RC load were varied to achieve diverse pulsation results. The final circuit design produced a circuit that had ten times the resolution and five times the sensitivity of previous NPS silicon controlled rectifier (SCR) based circuits. Additionally, the circuit in this thesis was able to detect AM-241 and CS-137 sources for the first time at NPS. Future NPS thesis research is proposed to further understand and fine-tune semi-conductor–based radiation detectors. It is proposed that future naval feasibility assessments be centered on the signal amplification and processing techniques from SCS-based circuits.

THIS PAGE INTENTIONALLY LEFT BLANK

TABLE OF CONTENTS

I. INTRODUCTION....1
- A. BACKGROUND, RECENT DEVELOPMENTS, AND POSSIBLE APPLICATIONS....1
- B. SCS-BASED CIRCUIT OPERATION....3
- C. IMPETUS FOR THESIS....5
- D. THESIS ORGANIZATION....5

II. EXPERIMENTAL ANALYSIS OF KEY CIRCUIT ELEMENTS....7
- A. SCS STANDALONE I-V OPERATION....7
- B. CONTROL OF I-V CHARACTERISTICS USING ZENER DIODE....8
- C. SCS FEEDBACK RESISTOR....11
- D. EFFECT OF LOAD RESISTOR ON THE SCS CIRCUIT....14

III. EXPERIMENTAL ANALYSIS OF ASSEMBLED CIRCUIT PULSE CHARACTERISTICS....17
- A. SCS CIRCUIT TRIGGERING FROM EXTERNAL BIAS....17
- B. CIRCUIT TRIGGERING FROM ANODE GATE CURRENT....20
- C. CIRCUIT TRIGGERING FROM LIGHT SOURCE....25
- D. CIRCUIT TRIGGERING FROM RADIATION SOURCES....26

IV. CONCLUSIONS AND RECOMMENDATIONS....31
- A. CONCLUSIONS....31
- B. RECOMMENDATIONS....32
- C. FEASIBILITY OF FUTURE NAVAL APPLICATIONS AND POSSIBLE FUTURE STUDIES....32

APPENDIX A. SEMICONDUCTOR DETECTOR DESIGN CRITERION WORK SHEET....35

APPENDIX B. CALIBRATION PROCEDURE....37

LIST OF REFERENCES....39

INITIAL DISTRIBUTION LIST....41

THIS PAGE INTENTIONALLY LEFT BLANK

LIST OF FIGURES

Figure 1. SCS-based Circuit with Photodiode Connected to the Anode Gate for Sensing Light and Ionizing Radiation 2

Figure 2. Measured Pulse Sequences under Three Different Intensities 2

Figure 3. Measured Pulse Sequences under Incidence from an Alpha Source 3

Figure 4. Logic Block Diagram of SCS Base Detector 4

Figure 5. Basic Electrical Component Schematic of SCS Base Detector 4

Figure 6. SCS (ECG-239) Standalone I-V Characteristic with Added Circuit Load Line 7

Figure 7. SCS Band Diagram under Forward Biased and Before Switching to the on State 9

Figure 8. SCS Band Diagram with Forward Biased and After Switching to on State 10

Figure 9. Portion of the Measured I-V Characteristics of the SCS (ECG-239) with Two Different Zener Diodes of Different Breakdown Voltages Connected Between the N_1 and P_2 11

Figure 10. I_H as a Function of R_F 12

Figure 11. I_H as a Function of R_F (22M-ohm and 44M-ohm) 12

Figure 12. Switching Voltage as a Function of R_F 13

Figure 13. Holding Current as a Function of R_F 13

Figure 14. Effect of Biasing on SCS (ECG239) with Zn (BR5231), R_F of 1.8MΩ R_L of 22MΩ and C of 3.5nF 18

Figure 15. Pulse Saturation for V_{SAT} R_F = 510kΩ and R_L = 1.51MΩ 19

Figure 16. Pulse Saturation for V_{SAT} R_F-5.1MΩ R_L-15.1MΩ 19

Figure 17. FDS100 Dark Current as a Function of Bias and Photocurrent under Illumination from Varied Light Intensities 22

Figure 18. Measured FDS100 Response as a Function of Bias When Exposed to AM-241 Source Along with the Dark Current 22

Figure 19. Measured FDS100 Response as a Function of Bias When Exposed to CS-137 Source Along with the Dark Current 23

Figure 20. SCS Pulsation from I_{AG} on R_F = 510 kΩ V_{BIAS} 2.111 V 24

Figure 21. SCS Pulsation from I_{AG} R_F = 5.1 MΩ V_{BIAS} 2.330 V 24

Figure 22. Photon Induced Pulse-Train for a Set of Light Levels on the Photodiode 25

Figure 23. PD Response When Exposed to CS-137 and AM-241 Radiation Sources 27
Figure 24. Response of Circuit under Dark Conditions 28
Figure 25. Response of Circuit When Exposed to AM-241 Source 28
Figure 26. Response of the Circuit exposed to CS-137 Source 29

LIST OF TABLES

Table 1. Summary of the PD Characteristics 23
Table 2. AM-241 Source Details 26
Table 3. CS-137 Source Details 27

THIS PAGE INTENTIONALLY LEFT BLANK

LIST OF ACRONYMS AND ABBREVIATIONS

AG	Anode Gate
C	Capacitor in RC-load
CG	Cathode Gate
DC	Direct Current
FOM	Figure of Merit
HFA	High Frequency Active
I_{AG}	Current Placed on the AG of the SCS
I_{DARK}	Constant PD Leakage Current
I_H	Holding Current
I_S	Switching Current
I-V	Current to Voltage Relationship
LiDAR	Light Detection and Ranging
NPS	Naval Postgraduate School
PD	Photodiode
RC	Resistor and Capacitor
RF	Feedback Resistor
RL	Load Resistor
SCR	Silicon-Controlled Rectifier
SCS	Silicon-Controlled Switch
SONAR	SOund Navigation and Ranging
V_{BIAS}	Applied Bias Voltage
V_H	Holding Voltage
V_S	Standalone SCS Switching Voltage
V_{SAT}	V_{BIAS} on the SCS Circuit
Zn	Zener Diode

THIS PAGE INTENTIONALLY LEFT BLANK

ACKNOWLEDGMENTS

I would first like to thank my thesis advisor Gamani Karunasiri and co-advisor Fabio Alves for their enthusiasm, diligence, and experience in guiding me through this thesis process.

I would also like to acknowledge Rear Admiral (Ret.) Winford (Jerry) Ellis, USN, chairman of the Naval Postgraduate School (NPS) Undersea Warfare Program, for his continuous support. Particularly, in providing me unparalleled access to the leaders of the Navy to present my thesis findings and its future naval feasibility studies to Naval Reactors and the Strategic Systems Program.

I would also like to thank Captain Hurt Rothenhaus, USN, Commanding Officer, SPAWAR, Systems Center Pacific for granting me the honor of being selected for the SPAWAR fellowship program. The access to the SPAWAR staff, in particular Dr. Joanna Ptasinski, provided great insight to current Navy studies and technical expertise.

Most of all I would like to thank my wife, the former Sheila Ann Bird, for making the NPS experience my most rewarding tour yet. Without question, the birth of our child, Willow Rayne Kjono, has been our greatest joy, and she keeps us centered as we embrace each other onto the next adventure.

THIS PAGE INTENTIONALLY LEFT BLANK

I. INTRODUCTION

A. BACKGROUND, RECENT DEVELOPMENTS, AND POSSIBLE APPLICATIONS

Current applications of ionizing radiation detection devices are heavily centered on the use of gas-amplification, scintillation crystals, or cryogenically cooled semiconductor-based systems. To operate these detection devices, complex auxiliary systems are required to achieve the dependable detectability of radiation. Utilizing solid P-N junction semiconductor devices dramatically reduces the required size of detector compared to substantially less dense gas systems [1]. Furthermore, harnessing semiconductor devices that have low leakage current at room temperature would remove the requirement of cryogenically cooling the device [2]. Additionally, achieving a device that can internally produce significant signal amplification would remove other auxiliary support needed.

"It was proposed that the silicon controlled switch (SCS) based radiation detector is potentially able to combine the advantages of the small size and low power consumption of semiconductor detectors, with the high gain and sensitivity of the gas detectors." [2, p.1] Previous research at Naval Postgraduate School (NPS) by Moore [3] and Casal [4] modeled and developed an understanding of the standalone SCS I-V characteristics and transition between on and off states. Additionally, Chang [5] analyzed in-depth the required circuit design parameters to allow for the generation of self-terminating pulses when the SCS is connected to a direct current (DC) bias and (resistor and capacitor connected in parallel) RC load.

SCS-based technology provides significant internal signal amplification from current producing sensors [2]. Figure 1 shows a typical SCS-based circuit along with a photodiode (PD) connected to the anode gate (AG) for sensing light and ionizing radiation. From previous NPS research it was noted that with an incident light on the order of μW, the circuit in Figure 1 produced 8 V pulse streams [6], as seen in Figure 2. Professors Fabio Alves, Craig Smith, and Gamani Karunasiri [2] provided insight on the initial SCS-based circuit that detected alpha particles, as seen in Figure 3, that shows that

there is high potential in the future study of semiconductor-based devices that can produce large signal amplification.

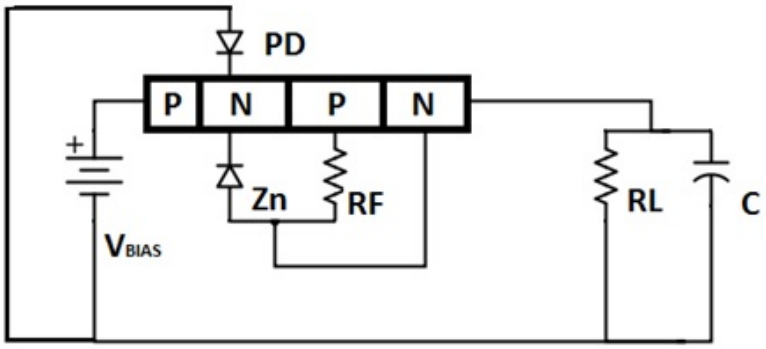

Figure 1. SCS-based Circuit with Photodiode Connected to the Anode Gate for Sensing Light and Ionizing Radiation

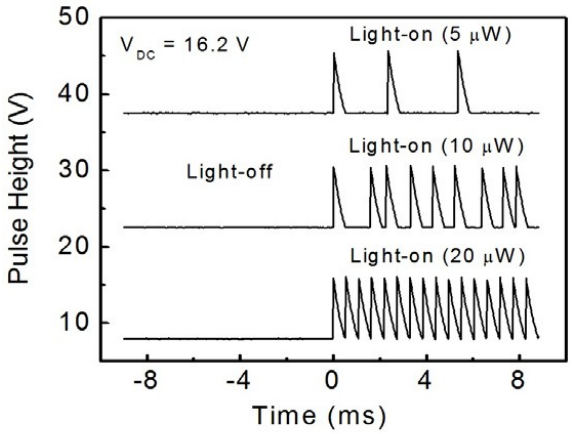

Figure 2. Measured Pulse Sequences under Three Different Intensities

Adapted from [6]: G. Karunasiri, "Spontaneous pulse generation using silicon controlled rectifier." Applied Physics Letters [Online], vol. 89, no. 2, p. 1. Available: http://scitation.aip.org/content/aip/journal/apl/89/2/10.1063/1.2220528

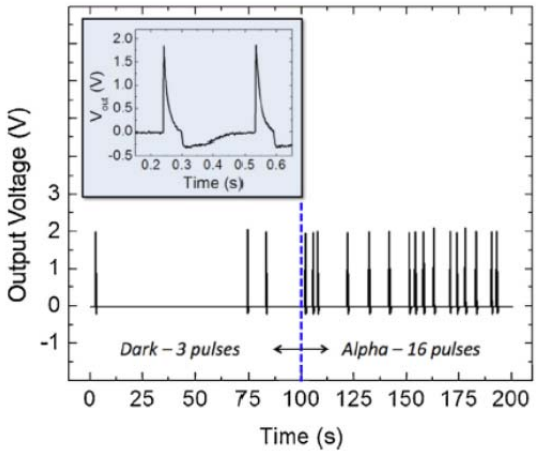

Figure 3. Measured Pulse Sequences under Incidence from an Alpha Source

Adapted from [6]: G. Karunasiri, "Spontaneous pulse generation using silicon controlled rectifier." Applied Physics Letters [Online], vol. 89, no. 2, p. 1. Available: http://scitation.aip.org/content/aip/journal/apl/89/2/10.1063/1.2220528

This work builds upon the previous findings for possible submarine warfare applications with a particular focus on gamma radiation detection systems. Figures 2 and 3 clearly show the future potential this approach has for detecting ionizing radiation. The difficulty in the future development toward detecting a gamma radiation is the ability for the detector to interact with the high energy gamma radiation.

B. SCS-BASED CIRCUIT OPERATION

The SCS-Based Detector is composed of three groups, which are: the sensing element, switching element, and output. The sensing element (red block in Figures 4 and 5) is composed of a photodiode (PD). The switching element (blue block in Figures 4 and 5) is composed of: a DC voltage source, SCS, Zener Diode (Zn) connected to the anode gate, and feedback resistor (R_F) connected to the cathode gate as shown Figure 5. The output (green block in Figures 4 and 5) is composed of an RC load. Voltage out is measured on the cathode of the SCS as the RC load dissipates the energy passed to it. We have chosen to add an oscilloscope to view pulses from the SCS circuit, as seen in Figure 5. These elements are combined in the manner displayed in the logic block diagram in Figure 4 and circuit layout in Figure 5.

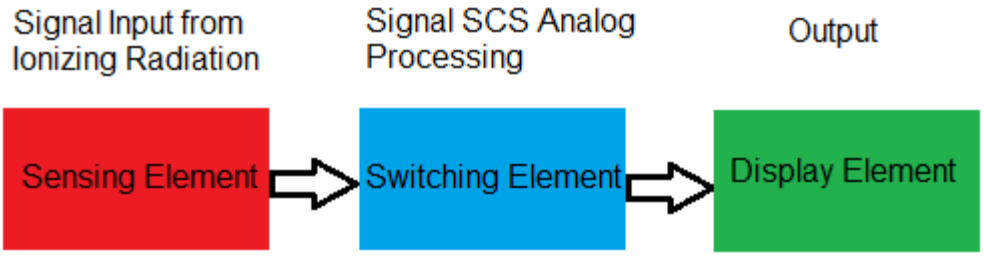

Figure 4. Logic Block Diagram of SCS Base Detector

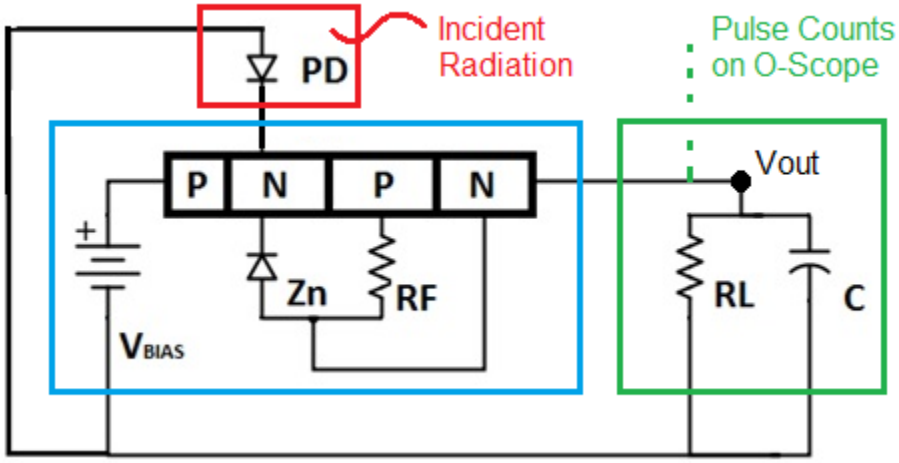

Figure 5. Basic Electrical Component Schematic of SCS Base Detector

The purpose of the DC bias (V_{BIAS}) is to place the operation point of the SCS as close as possible to its switching voltage [2] in order to allow minute stimulus to switch the SCS between its "on" and "off" states. When there is no current injection in the cathode gate of the SCS, or current drain on the anode gate, the SCS remains in its high impedance mode, functioning as an open path in the circuit. The photodiode is responsible for detecting light/radiation and upon detection, drain current from the SCS anode gate to allow switching to the conduction mode, functioning as a closed path in the circuit. The RC load is responsible for switching the SCS back to its high impedance "off" state. At this point, if the stimulus remains, the SCS will switch to its conduction mode ("on" state) and back repeatedly, generating a stream of pulses. When the stimulus

is ceased, the pulse stream is terminated. A detailed explanation on how this circuit works is given in Chang's thesis [5].

C. IMPETUS FOR THESIS

The objective of this thesis is to probe the potential of an SCS-based pulse generating circuit for detection of gamma radiation. The circuit is made with only commercial-of-the-shelf (COTS) components. In-order to achieve this intent, it is necessary to understand how the photodiode responds to ionizing radiation to generate trigger current for the circuit, and how to best use individual components to fine-tune the switching characteristics for generating pulses with extremely low trigger current levels.

It is important to select a photodiode that interacts efficiently with radiation and has a low dark current for operation at room temperature. In addition, the circuit components that modify the SCS I-V characteristics, and consequently the overall sensitivity of the circuit, needs to be investigated. In this work, the components for an SCS-based pulse generating circuit to detect gamma radiation are examined and properly selected in order to produce the best pulse response characteristics for a given anode gate current.

D. THESIS ORGANIZATION

The rest of thesis is organized in the following manner:

Chapter II describes the individual components employed as well as the assembled circuit's behavior. Particular attention is given on the understanding of how the I-V characteristic of the SCS is affected by the individual circuit components. This will allow the optimization of the circuit for the detection of gamma and beta rays from CS-137 radioactive source available at NPS.

Chapter III includes the analysis and description of the pulse-generating capability of the circuit under stimuli from light and radiation sources (AM-241 and CS-137). Particular attention is given to describing the generated current in the photodiode from the influence of various radiation fields and the ability of a given circuit to provide a proportional output to characterize the incident field.

Chapter IV describes the results obtained using the optimized circuit and summarizes the key conclusions drawn from this work. Additionally, the benefits and limitations of the developed circuit are explained to provide insight into future research work as well as possible immediate applications.

II. EXPERIMENTAL ANALYSIS OF KEY CIRCUIT ELEMENTS

A. SCS STANDALONE I-V OPERATION

A Silicon-Controlled Switch (SCS) is a semiconductor device that transitions from a high impedance mode (high voltage and low current) to a conduction mode (low voltage and high current) as shown in Figure 6. The main advantage of using an SCS for ionizing radiation detection is the ability to sense very weak signal/stimulus through the switching of SCS states. Since the output can be many orders of magnitude higher than the stimulus signal, this phenomenon can be interpreted as an amplification process.

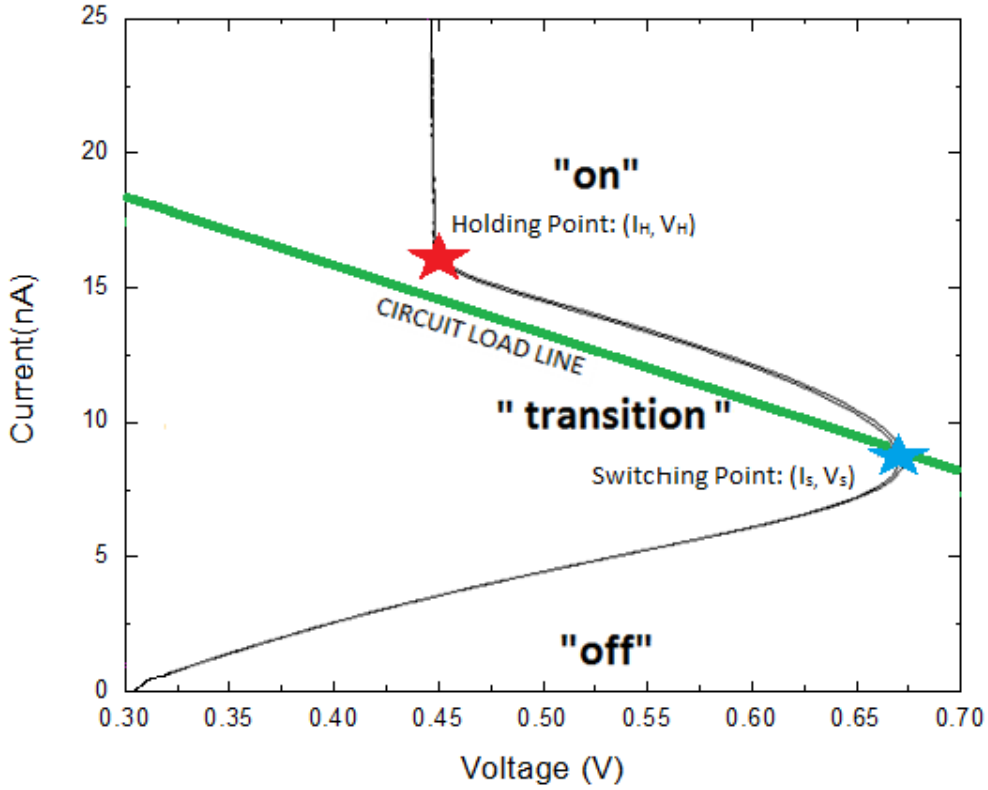

Figure 6. SCS (ECG-239) Standalone I-V Characteristic with Added Circuit Load Line

The important points on the I-V characteristic shown in Figure 6 are the switching point and holding point. The switching point is located at the associated switching

voltage (V_S), and switching current (I_S), found in Figure 6 at (V= 0.7 V, I =10 nA). The holding point is at the associated holding voltage (V_H), and holding current (I_H), found in Figure 6 at (V = 0.45 V, I = 20 nA). As current increases above I_S, the device starts to transition from its "off" to "on" state. To utilize the SCS transition region, currents lower than I_S and greater than I_H are not allowed, as per the selected circuit components. In order to obtain self-terminating pulses, the SCS must be connected with reactive and resistive load (parallel RC load) and the bias must be adjusted to place the load line as shown by the solid green line in Figure 6. A comprehensive explanation of placing the load line can be found in [5]. When a photodetector is connected to the SCS anode gate, the current generated by the detector due to illumination (light/radiation) will alter the I-V characteristic of the SCS, forcing it to switch from off state to the on state. If the SCS is biased to the correct operating point, the circuit outputs pulses. It was observed that the pulse rate is proportional to the gate current until saturation occurs [1]. The pulse duration is determined by the RC time constant of the load. The maximum pulse rate is limited by the RC time constant. If there are 2 stimuli within the duration of one pulse, only one pulse will be generated.

B. CONTROL OF I-V CHARACTERISTICS USING ZENER DIODE

In order to understand the effects of the Zener diode (Zn) on the I-V characteristics of the circuit, a brief review of the SCS physics is necessary. The SCS is a four layer P_1-N_1-P_2-N_2 semiconductor device. Figures 7 and 8 shows the schematic energy band diagrams of a SCS before and after switching, respectively. There are three P-N junctions; P_1-N_1, N_1-P_2 and P_2-N_2 junctions, which are usually denoted by junction one, two, and three, respectively. When a forward bias is applied across the SCS, junctions one and three will be forward biased (resulting in a lower internal electric field) while the middle junction will be reverse biased (resulting in an greater internal electric field), as seen in Figure 7, keeping the SCS in its off state.

The resultant band diagram generates two potential wells for electrons (at the junction one) and for holes (at the junction three). Under forward bias, the two outer junctions inject electrons and holes in to the middle junction, which accumulate in the

two potential wells as illustrated in Figure 7, which keeps the SCS in the off state. The field generated by the accumulated charges is in opposition direction to the field due to the applied bias, which reduces the net electric field in the middle junction. As the accumulation increases the net internal field reduces to almost zero as seen in Figure 8 making the all three junctions forward biased. The net electric field in second junction decreases switching the SCS to the on state. As discussed above, the current will then flow through the SCS and be discharged by the RC load, providing negative feedback and returning to the "off" state [1].

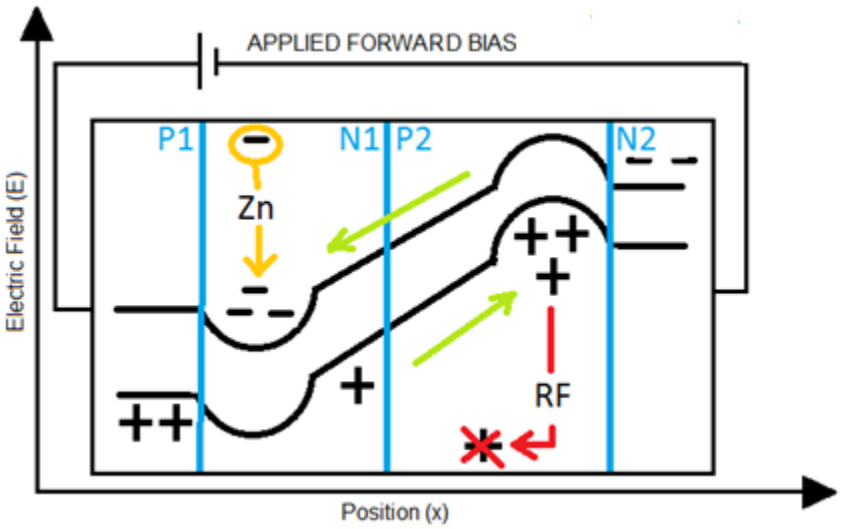

Figure 7. SCS Band Diagram under Forward Biased and Before Switching to the on State

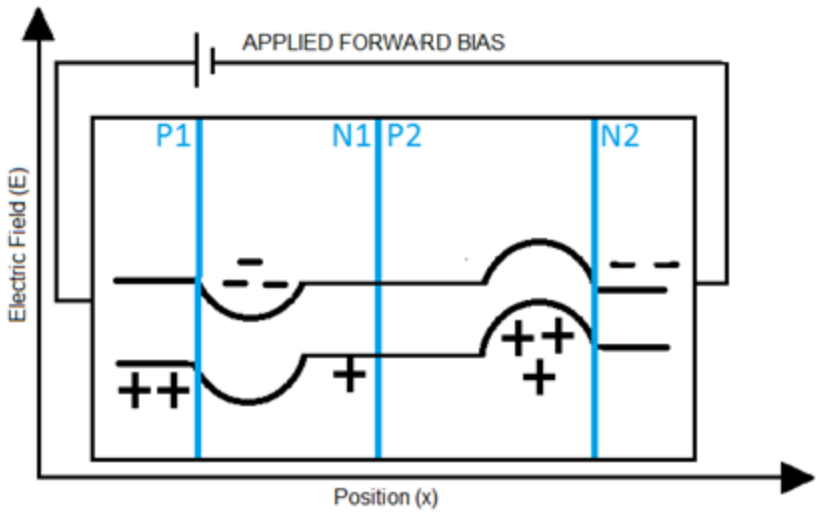

Figure 8. SCS Band Diagram with Forward Biased and After Switching to on State

Addition of the Zener diode between anode gate and cathode of SCS has the primary effect on the switching voltage (V_S) of the SCS since the conduction begins at the breakdown voltage of Zn if it is less than the V_S. This means that the Zn is connected to the circuit such that is operating under a reverse bias. The effect of this is the clipping of the voltage across the N_1 layer, while forcing the I-V characteristics of the SCS (solid lines) to follow the corresponding Zener I-V characteristics (dotted lines) shown in Figure 9. In effect, the adding of Zn moves V_s toward left relative to the intrinsic SCS I-V curve as the Zn breakdown voltage reduces. The trend in Zn breakdown voltages, matches previous theoretical analysis by Casal as it correlates to models that vary N_1 doping concentrations [4]. Furthermore, it confirms Moore's conclusions on thyristor switching with N_1 layer width, as found in [3].

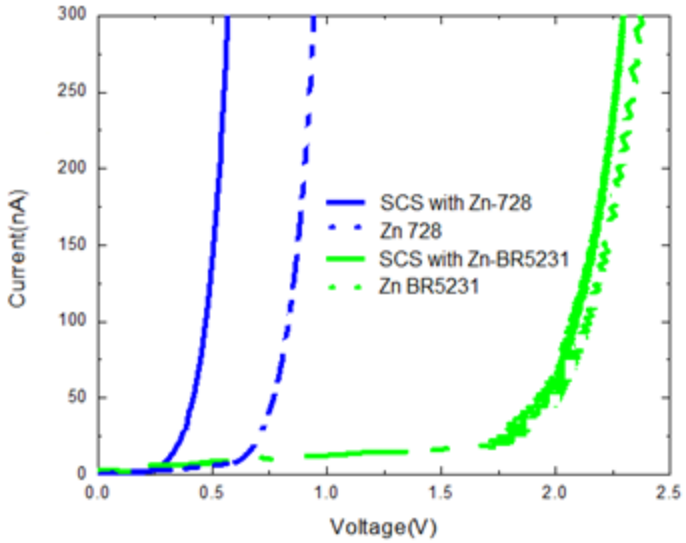

Figure 9. Portion of the Measured I-V Characteristics of the SCS (ECG-239) with Two Different Zener Diodes of Different Breakdown Voltages Connected Between the N_1 and P_2

To increase the sensitivity of our circuit we decided to lower the V_s. To ensure and track our operating parameters we measured the Zn as an individual element, and as a coupled device to the SCS with a R_F, as seen in Figure 9 for a fixed R_F of 1.5 MΩ. (Note: when the SCS wired only to a Zn, it will over-ride the field in the middle junction and acts as a reverse biased P-N diode, vice a SCS.) The switching voltages in Figure 9 were very close but not exactly matched to the associated Zn breakdown voltages. It was noticed that the V_s did closely match for the Zn with high breakdown voltage. In the case of the Zn with lower breakdown voltage, the new V_s did not match the Zn I-V curve.

C. SCS FEEDBACK RESISTOR

Incorporation of a feedback resistor (R_F) can aid in shifting the holding current (I_H) of the SCS. The R_F is connected between the SCS cathode gate (CG) and the cathode. Figures 10 and 11 show effect of R_F on the I-V characteristics of the SCR with a Zn attached to it. R_F regulates the loss of holes in the potential well formed at the third junction by flowing them to the cathode. As the R_F is decreased more holes will flow to the cathode, which reduces the accumulation of holes in the potential well requiring

higher DC bias to switch the SCR as seen in Figure 10. In effect, as R_F is reduced, it increases switching current (I_S) and holding current (I_H), requiring higher gate current to trigger the SCR. The magnitude of this effect of on SCS current can be seen between a standalone SCS I-V where fA are recorded for I_H, vice the SCS I-V curve seen in Figure 10, where nA are recorded for I_H.

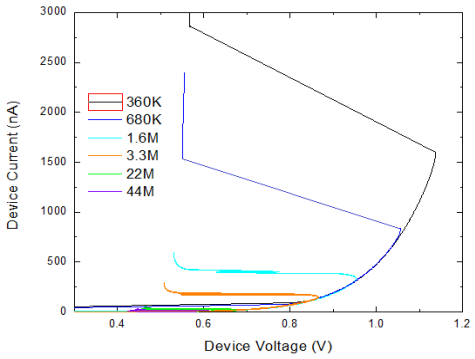

Figure 10. I_H as a Function of R_F

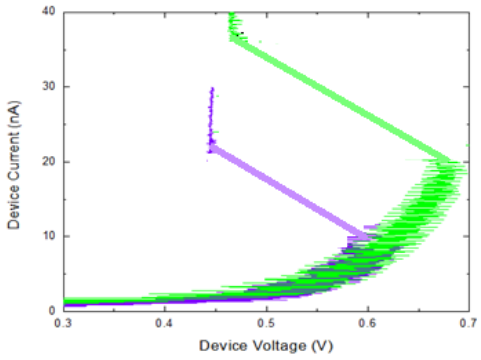

Figure 11. I_H as a Function of R_F (22M-ohm and 44M-ohm)

It was found that the dependence of V_S on R_F followed a log-linear pattern as seen in Figure 12, giving a linear fit was closely matched with a R^2=0.994 [R2 is defined as the weighted sum of the difference between the theoretical line and the experimental data points]. It was also found that the dependence of I_H on R_F followed a log-log pattern as seen in Figure 13, giving a linear fit was closely matched with a R^2=0.996.

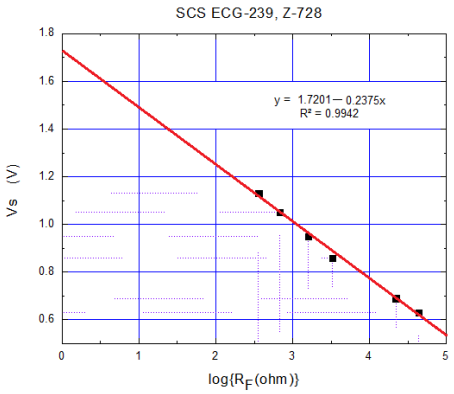

Figure 12. Switching Voltage as a Function of R_F

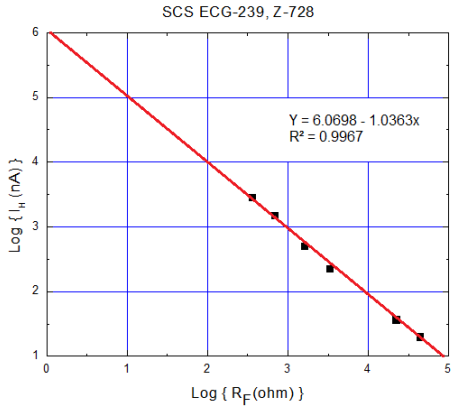

Figure 13. Holding Current as a Function of R_F

The correlation of R_F to I_H confirms previous conclusions made by Casal [4]. Through computer modeling Casal determined "The switching current, on the other hand, will likely be most affected by P_1 and N_2 doping since these layers contribute the most to the potential wells formed at N_1 and P_2" [4]. In our laboratory experiments, reduction of R_F allowed for the leakage of holes from the P_2 layer weakening the potential well formed on the third barrier junction. This has the same effect as reducing the doped concentration on P_1 and N_2. After detailed analysis with multiple data regression techniques, the relationship between R_F and the slope of the negative resistance region showed no simple correlation.

D. EFFECT OF LOAD RESISTOR ON THE SCS CIRCUIT

Figure 6 shows the I-V characteristics of an optimized SCS with Zn (728) and RF (10 MΩ) along with load line corresponds to R_L of 42 MΩ. The R_L regulates the slope of load line as well as the RC time constant of the circuit. Selection of R_L is important to set the conditions for generating pulses. The current through the circuit should be larger than the switching current (I_S) while smaller than the holding current (I_H) to prevent the SCS staying on. For application involving external stimulus, R_L must be large enough to prevent the SCS from reaching its required switching current (I_S) when the stimulus is not present [5]. An in-depth explanation of this and further explanation of pulse mode operation of SCS (I_S) can be found in [5].

The effect of load resistance on the circuit was explored by varying the R_L from 360 kΩ to 44 MΩ. As a practical design limitation to achieve pulsing, R_F:R_L ratio was maintained between 1:3 (typical V_S ~3V) and 1:5 (typical V_S ~9V). It was found that when R_F:R_L dropped below 1:3 pulsation was difficult to achieve. As R_F:R_L is increased the required biasing prior to pulsation is increased as well. To maintain sensitivity of the circuit R_F:R_L was maintained near 1:3. As the circuit was made more sensitive, selection of power supplies for biasing become vitally important as the calibration process took place on the mV scale. It was noted the higher R_F:R_L provided greater accuracy dead time between individual pulses and therefore a larger band of pulse rates prior to saturation. While R_L as allowed to vary, the capacitor was fixed at 3.3 nF to simplify circuit analysis.

It is important to state that the pulse duration depends on the RC time constant as the capacitor is discharged through R_L. The functional purpose of the capacitor was to set conditions for self-terminating pulses. In the RC load, the capacitor charges and induces a negative bias across the SCS to prevent it from reaching the I_H point and turning fully on, switching the SCS to the off state [5]. The time constant ($\tau=R_L*C$) is a measure of time it takes the capacitor to discharge to 63.2% from its peak value. The time constant varied from 1.19 ms to 145 ms for R_L values of 360 kΩ and 44 MΩ respectively, with a fixed capacitance of 3.3 nF. This time constant is functionally seen by the operator of the device as a window of time where more than one stimulus on the PD is seen as a singular pulse on the oscilloscope. Logically, this means that smaller time constants increases the

temporal accuracy of the detecting circuit. The optimized circuit used a 1.5 MΩ R_L, which yielded a $\tau = 4.9$ ms, which reduced the time constant of previous NPS design ($\tau =$ 49 ms) found in [2], by an order of magnitude. It was found that the premise of the selection of RC combination must reduce the dead time of the circuit, while being able to produce enough of a reverse current to switch the SCS off state [5].

THIS PAGE INTENTIONALLY LEFT BLANK

III. EXPERIMENTAL ANALYSIS OF ASSEMBLED CIRCUIT PULSE CHARACTERISTICS

A. SCS CIRCUIT TRIGGERING FROM EXTERNAL BIAS

Proper setup of the circuit will yield self-terminating pulses by either biasing (V_{BIAS}) the SCS, or stimulating the photodetector to produce trigger current (I_{AG}). Pulsation occurs as V_{BIAS} is raised enough to bring the current through the SCS near the switching current. The physics of this mechanism are summarized in paragraph II.B and discussed in detail in [5].

First, we studied the circuit response with only stimulation from V_{BIAS}. For V_{BIAS}, it was found the R_F:R_L ratio was key in setting the required V_{BIAS} to induce pulses. When R_F:R_L ratio was large, greater V_{BIAS} was required to induce pulsing. In order to create a more sensitive circuit (i.e., lower trigger current), with an RC load that allowed for self-terminating pulses an R_F:R_L ratio of 1:3 was set, with the R_F set to 1.5 MΩ. The greatest difficulty in operating such a sensitive circuit was controlling the biasing precisely on the mV scale. This required voltage control within 0.04%. For circuits with higher R_F:R_L ratios and V_S, tuning was much less restrictive as 0.01V control of V_{BIAS} at 9 V requiring voltage control within 0.1%. The strict requirements required controlling V_{BIAS} in tenths of mV at low voltages proves to be a great challenge for current research and future device implementation.

Control of V_{BIAS} above V_S resulted in interesting effects on the pulse stream. When V_{BIAS} was raised above V_S for the circuit, the number or pulses increased proportionally to V_{BIAS} until saturation imposed by the RC time constant. As seen in Figure 14, this functionally means there is a maximum pulse rate as stimulus strength is varied. This is as expected as the normal response for inducing a stronger field within the SCS by raising V_{BIAS} or PD stimulation does induce higher switching rates within the SCS to pass energy to the RC load.

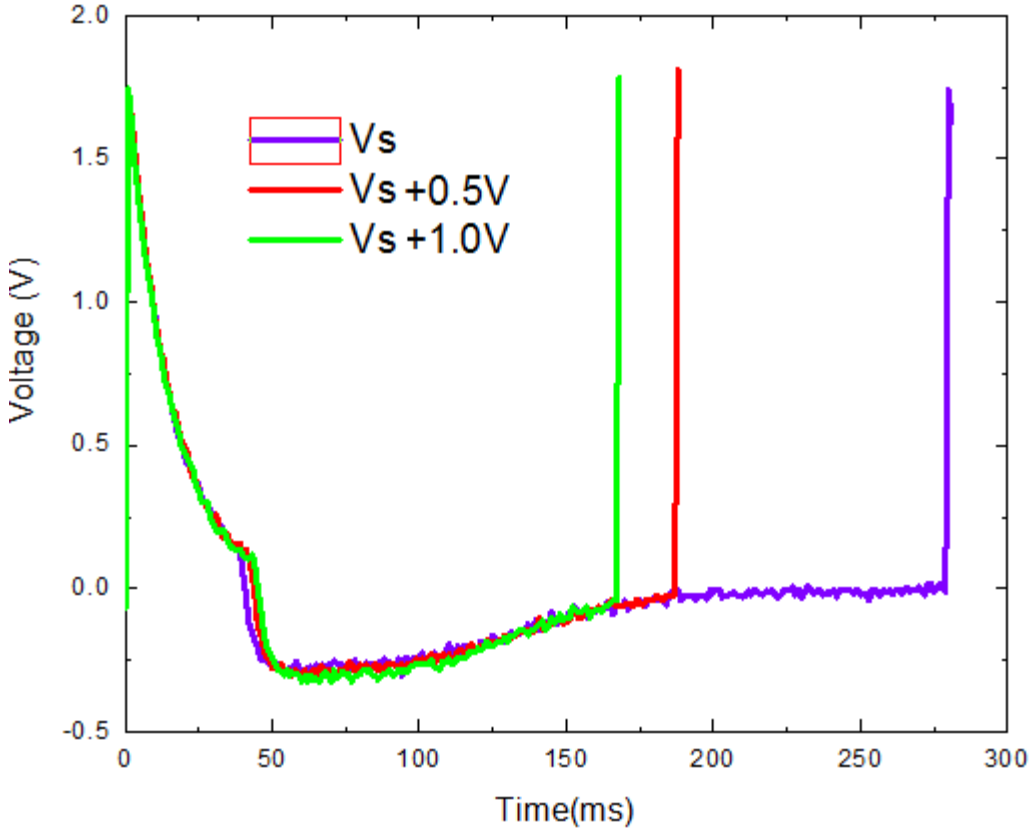

Figure 14. Effect of Biasing on SCS (ECG239) with Zn (BR5231), R_F of 1.8MΩ R_L of 22MΩ and C of 3.5nF

However, when the current on the SCS is larger than the holding current, the RC load cannot completely dissipate, and "pulse clipping" occurs as the RC load with receive energy from SCS returning to the on state prior to dissipating all the energy from the previous SCS pulse. This is when one pulse begins to cover the other pulses near it. Effectively the pulse count will pass a saturation point (V_{SAT}) and then decrease pulse counts as V_{BIAS} in increased. Figure 15 and 16 show the saturation of pulse rate for two distinct circuits.

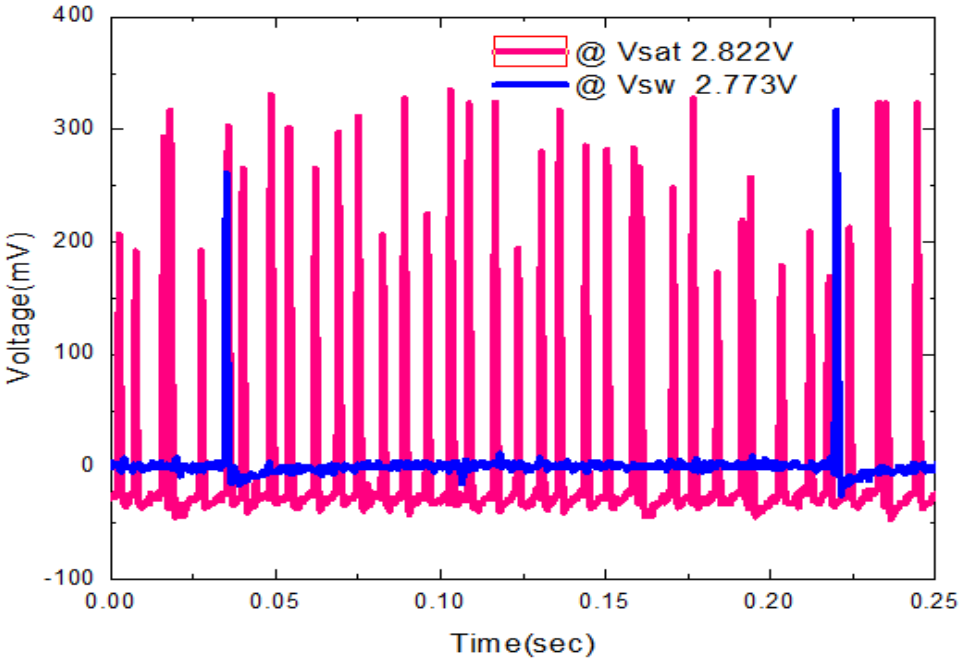

Figure 15. Pulse Saturation for V_{SAT} R_F = 510kΩ and R_L = 1.51MΩ

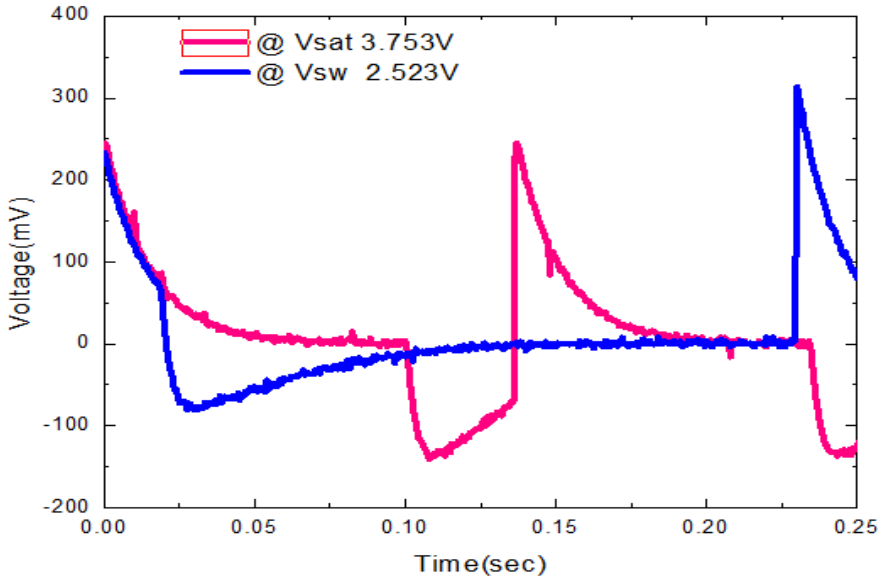

Figure 16. Pulse Saturation for V_{SAT} R_F-5.1MΩ R_L-15.1MΩ

A detailed measurement was carried out to quantify the saturation effects for a circuit with a high RF:RL of 1:6 with switching voltage (VS) of 8.68 V. Continuous pulsation was observed when a bias of 8.81 V was applied. This resulted in 230 ms

between continuous pulses with about 50 ms of dead time between pulses. As VBIAS was increased the dead time between pulses diminished. At 9.32 V the time between pulses was 190 ms with only 20 ms of dead time observed. Bias was increased until a constant output frequency was observed between pulses. Pulse saturation occurred at about 9.52 V with 165 ms between pulses, with no dead time between consecutive pulses. Biasing beyond this point resulted in no change of observed output frequency. When very high VBIAS (roughly twice the value of VS) placed on the SCS "pulse deletion" occurs. The SCS remains in the on state and no further pulses are seen since current through the SCS exceeded the holding voltage.

B. CIRCUIT TRIGGERING FROM ANODE GATE CURRENT

Measuring the effect of current injected into the AG of the SCS (I_{AG}) was probed to determine the current needed for triggering the SCS with optimized circuit components. The injection of current to the AG was achieved using a photodiode connected to it in the reverse bias mode and shinning different amount of light generate current. In order to generate pulses, the circuit required the presence of V_{BIAS} as well as I_{AG}. I_{AG} alone would not generate pulses, since the SCS needs to be near the switching point for generating pulses. With the presence of I_{AG}, the switching occurs at a lower voltage due to injection of holes from the AG to the P2 layer and corresponding V_{BIAS} can also be reduced [5]. Initially, the photodetector characteristics were analyzed so that I_{AG} limits could be properly understood.

Some of the PDs chosen to study where two photodiodes FDS100 (silicon) and FGAP71 (gallium phosphate). The FDS100, which was analyzed previously by the NPS Sensor Research Laboratory and used in a SCS circuit for detecting AM-241 and CS-137 sources, as seen in [2]. The FGAP71 was purchased to experiment with as the semiconductor GaP, which has larger bandgap (lower dark current) and was presumed to be more suitable to detect ionizing radiation sources due to its higher molecular weight (high-Z) compared to the silicon-based FDS100. The protective windows of the detectors were removed to ensure alpha particles interact with the sensing element.

An interesting unanticipated effect of connecting the PD to the AG of the SCS was the impact of the PD dark current (I_{DARK}) on V_S. The thermally generated dark current from the PD found to switch the SCS at a lower V_S than originally anticipated. This is due to the injection of hole to the gate terminal, which sped up the switching process. Figure 17 shows measured dark and photocurrent of FD100 photodiode as a function of bias for a set of light intensities from 2.5 to 25 nW using Agilent 4155 semiconductor parameter analyzer. The measured currents were between 5–15 nA. Figures 18 and 19 show current generated by FD100 when exposed to AM-241 and CS-137 sources, respectively along with the measured dark current. The FGAP71 only provided a limited response, most likely due to its extremely thin depletion layer thickness, approximately l~.5 μm though the sensing element is made of high-Z material. While FDS100 was made of silicon (a lower molecular weighted element that is less likely to react with the incident radiation) but the thickness of the depletion layer was roughly 50 times the thickness of the FGAP71 at ~25 μm. This provided a much larger region of interaction to form electron-hole pairs to produce higher I_{AG}. Table 1 shows a summary of the photo detector measurements. Based on the data in Figures 18 and 19, the two radioactive sources generated current in the range of 80 pA to 110 pA. Based on the measurements, the FDS100 was selected as the trigger generator due to its better performance.

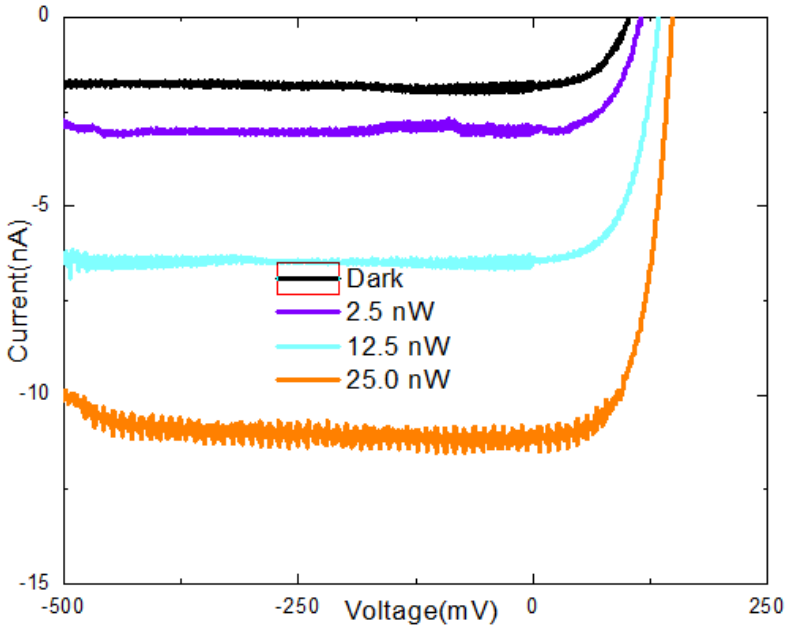

Figure 17. FDS100 Dark Current as a Function of Bias and Photocurrent under Illumination from Varied Light Intensities

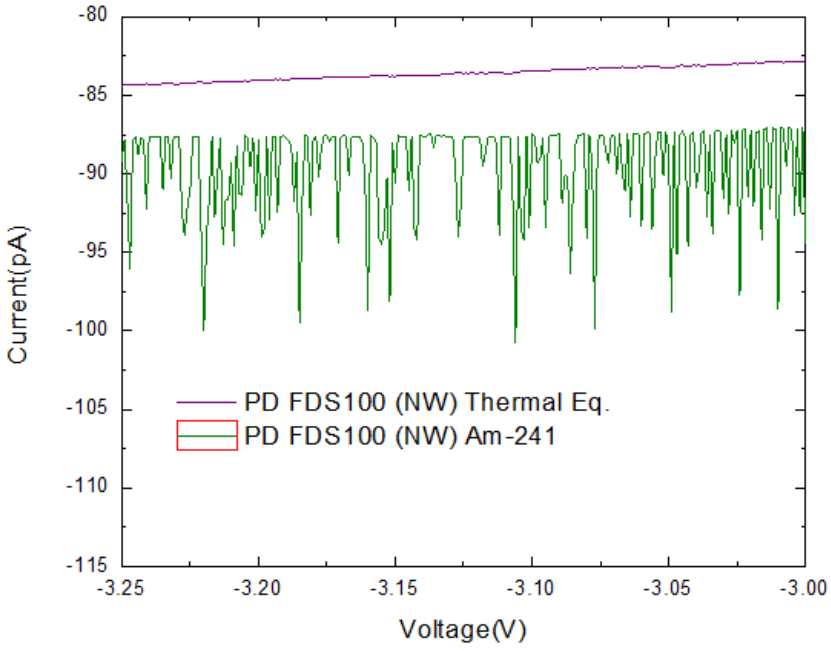

Figure 18. Measured FDS100 Response as a Function of Bias When Exposed to AM-241 Source Along with the Dark Current

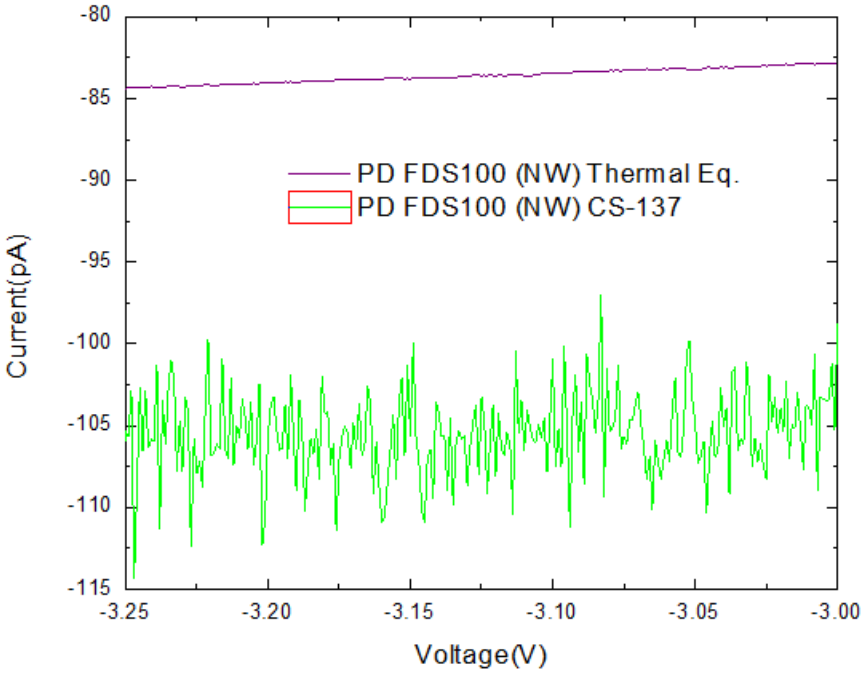

Figure 19. Measured FDS100 Response as a Function of Bias When Exposed to CS-137 Source Along with the Dark Current

	FDS100	FGAP71
I_{DARK}	- 2 nA	- 50 pA
ΔI_{LIGHT}	3/5/10 nA	-
ΔI_{AM-241}	15 pA	1 pA
ΔI_{CS-137}	20 pA	.5nA
Area	13 mm^2	4.84 mm^2
Material	Si	GaP
ℜ	.6 A/W	.12 A/W

Table 1. Summary of the PD Characteristics

To measure how pulsation would respond to a range of I_{AG} and produce a metered response the analysis was setup in the following manner. V_{BIAS} is set to a voltage where pulsation would first occur and I_{AG} of -80 pA is applied on the SCS from an AGILENT 4155B Parameter Analyzer. At this point, the counts from pulsation and V_{BIAS} are recorded. After this, a larger I_{AG} of -110 pA is applied on the SCS anode gate while

maintaining the same V_{BIAS}. The counts are then recorded. As seen in Figures 20 and 21, the SCS circuit outputs correspond to two different feedback resistors. The pulse rate as expected has a strong correlation to the magnitude of I_{AG}, and therefore the intensity of incident source. It is important to also note that V_S is significantly lower when any I_{AG} is applied on the SCS. It was observed that when the V_{BIAS} or I_{AG} is adjusted, circuits initially generated burst of pulses (see Figure 20), which could be due to triggering of SCS by sudden change in bias or trigger current.

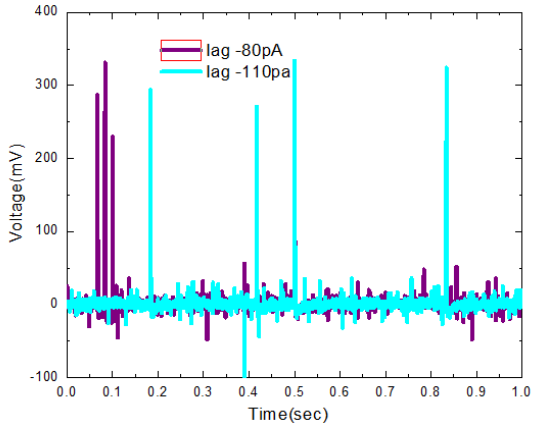

Figure 20. SCS Pulsation from I_{AG} on R_F = 510 kΩ V_{BIAS} 2.111 V

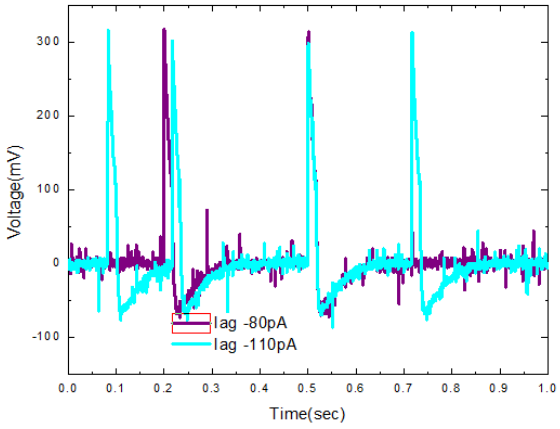

Figure 21. SCS Pulsation from I_{AG} R_F = 5.1 MΩ V_{BIAS} 2.330 V

C. CIRCUIT TRIGGERING FROM LIGHT SOURCE

It was found that the "pulse rate was highly sensitive to the dc bias and could also be controlled by directly injecting current through the gate terminal of the SCR." [6, p. 1] This reference is used as the premise to develop further research in the ability to generate self-terminating pulse trains. In this original design the PD was stimulated by light to produce the I_{AG}.

As seen in Figure 22, the circuit responded with varied pulse counts as the incident light was varied on the PD. This proved the concept that for our final design the calibration of the circuit could provide a metered response to measure the incident radiation on the PD. Figure 22 shows the response of the circuit as the exposure to the ambient light is varied. As the PD was enclosed in metal box, we placed a varied number of stacked washers to shim open the cover to this box. This allowed us to vary the incident power levels on the PD as indicated in Figure 22. It was found that circuit was extremely sensitive light detector and pulse rate saturated at around 25 nW.

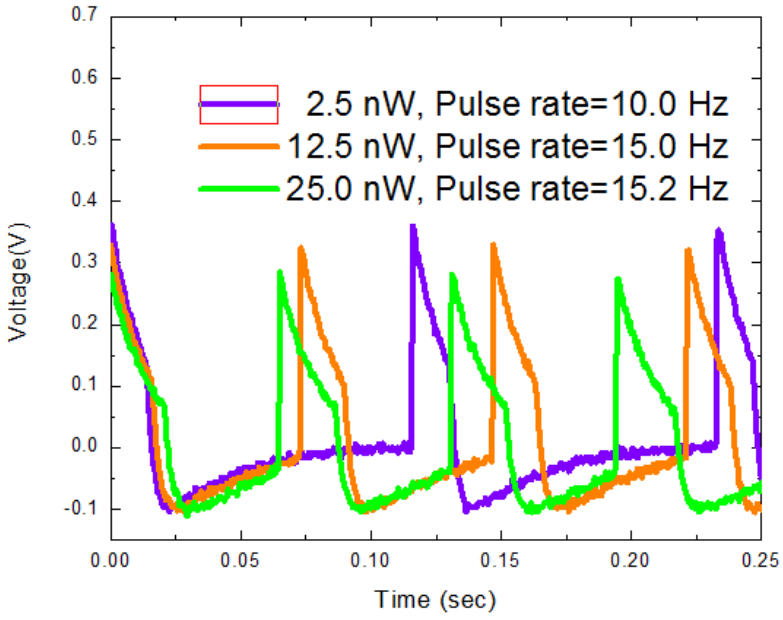

Figure 22. Photon Induced Pulse-Train for a Set of Light Levels on the Photodiode

D. CIRCUIT TRIGGERING FROM RADIATION SOURCES

Interaction of ionizing radiation with materials generates charged particles such as electrons through either the photoelectric effect, electron pair production or Compton scattering [1]. The interaction of ionizing radiation with semiconductors generate electron-hole pairs with amount depends on the type of radiation. Initial measurements were carried out determine interaction of radiation with the photodiode. The PD FDS100 was placed in the Agilent 4155B parameter analyzer while the I-V curve of the PD with no stimulation from light or radioactive sources was determined. Then the respective source was placed on the PD and a second I-V curve of the PD was collected. Figure 22 shows measured responses of the FDS100 photodiode using Agilent 4145 semiconductor parameter analyzer when exposed to beta and gamma radiation from a CS-137 source and alpha particles from AM-241 source. The source is inherently different and produces a fundamentally different I-V characteristic in the PD. AM-241 produces heavy slow moving alpha particles that deposit all of its energy within the active region of the PD. The CS-137 generates fast beta and gamma radiation depositing some of their energies within the detector due to the smaller interaction cross section. Figure 23 shows higher average current due to the CS-137 compared to that of AM-241 probably due to different radiation fluxes from the two sources. It can be seen that the interaction of alpha particles generate larger current spike due to depositing most of energy with in the active region. Tables 2 and 3 respectively summarize the AM-241 and CS-137 sources used in this thesis.

	K-eV	Percent
Gamma	60	36
Beta	N/A	N/A
Alpha	5486	85
	5443	13
1/2 Life	432.7	Years
Activity	3.43	Ci/g

Table 2. AM-241 Source Details

Adapted from [7] Radiation Safety Department. (n.d.). University of Cincinnati. [Online]. Available: http://researchcompliance.uc.edu/radsafety.aspx. Accessed Oct. 30, 2015.

	K-eV	Percent
Gamma	662	85
Beta	173	5
	512	95
Alpha	N/A	N/A
1/2 Life	30.2	Years
Activity	87	Ci/g

Table 3. CS-137 Source Details

Adapted from [7] Radiation Safety Department. (n.d.). University of Cincinnati. [Online]. Available: http://researchcompliance.uc.edu/radsafety.aspx. Accessed Oct. 30, 2015.

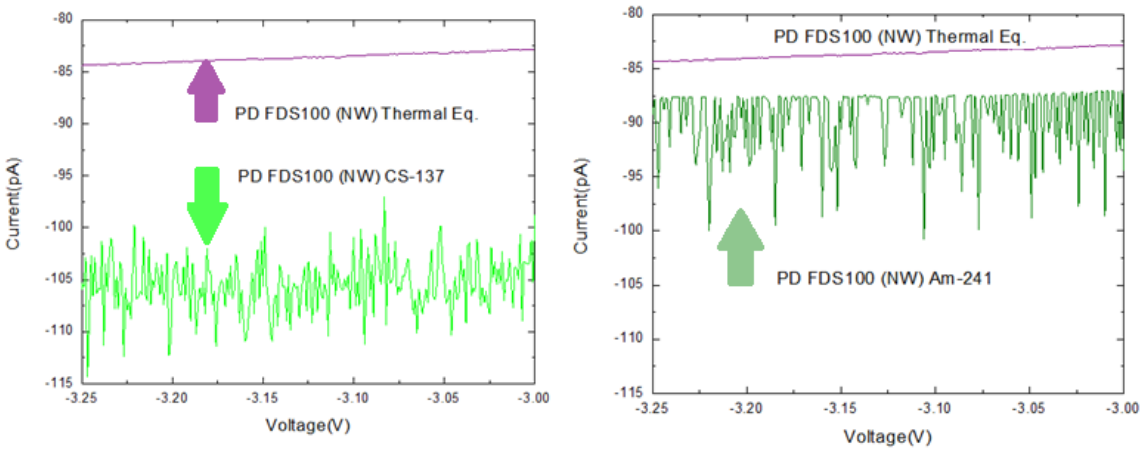

Figure 23. PD Response When Exposed to CS-137 and AM-241 Radiation Sources

The previous NPS design proved the feasibility of detecting alpha emission using a similar approach [2]. That design produced on average, 19 pulses over 190 seconds from an AM-241 source. This yielded a pulse rate of 0.1 pulses/sec. The same source was later used to test our optimized detection circuit that produced an average pulse rate of 0.45 pulses/sec. This showed the circuit to be slightly less than 5 times better, regarding the temporal response toward alpha particles. Furthermore, a response of 1.2 pulse/sec was determined when exposed to CS-137 source. Figure 24 through 26 shows the circuit output under dark conditions as well as under the stimulation using AM-241 and CS-137 sources. The pulse heights are different due to the low resolution of the slow time base

used to capture the signals. At present, it is not clear the SCS-Based Detector can detect sources that emit only gamma radiation since the CS-137 source produces both beta and gamma radiation.

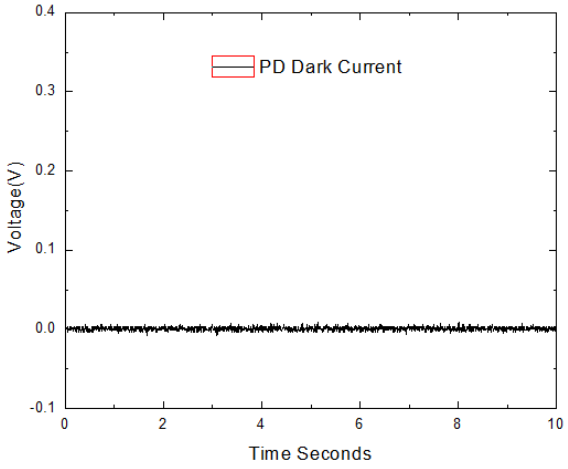

Figure 24. Response of Circuit under Dark Conditions

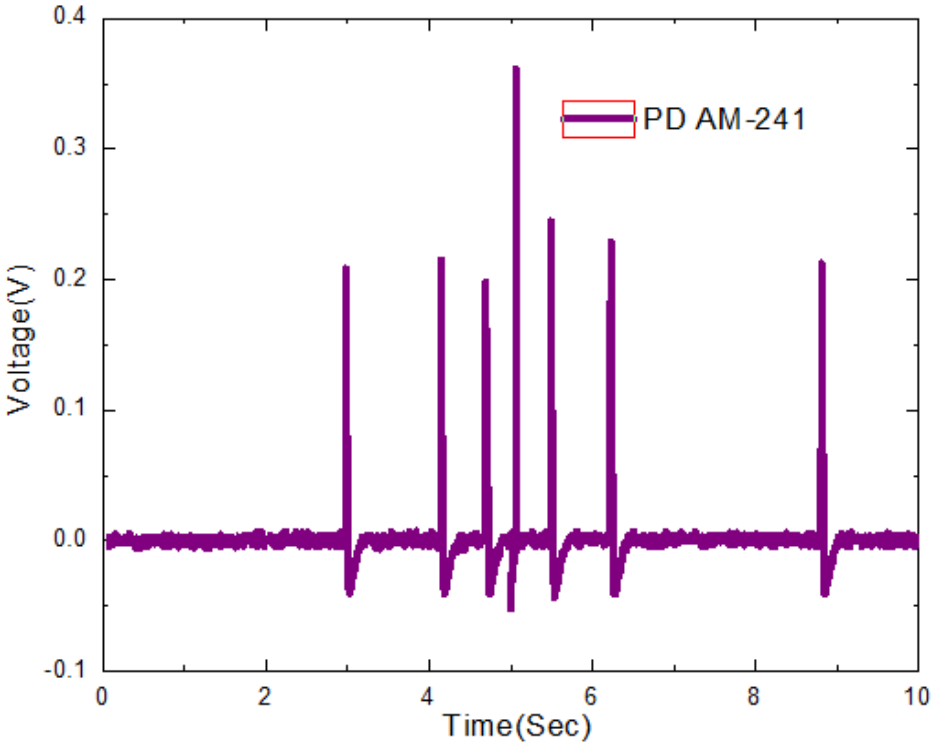

Figure 25. Response of Circuit When Exposed to AM-241 Source

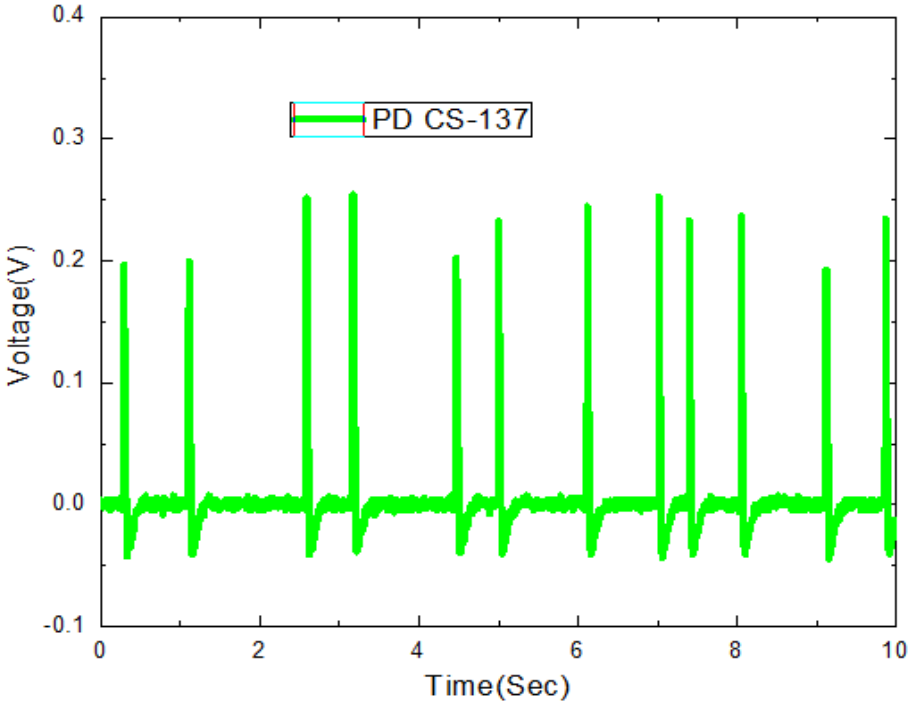

Figure 26. Response of the Circuit exposed to CS-137 Source

THIS PAGE INTENTIONALLY LEFT BLANK

IV. CONCLUSIONS AND RECOMMENDATIONS

A. CONCLUSIONS

The purpose of this thesis was to utilize the existing NPS knowledge of pulse mode radiation detection using SCS-based circuits. Primary goal was to detect radiation from key a CS-137 sources with improved pulse rate.

The SCS-based circuit was optimized by the selection of feedback to load resistance ratio to be around 1:3 and a switching voltage between 2–3 volts. Relatively large values of feedback and load resistor values where used to create a circuit with low trigger current to enhance the sensitivity. When circuits where built with low feedback to load resistance ratio, or large feedback resistor values, bias voltage control on the mV scale was required to tune the circuit for achieving high sensitivity. The SCS I-V curve we optimized by adding feedback resistor and Zener diode to the SCS, which allowed the reduction of trigger current for generating pulsed by many orders of magnitude.

Empirical relationships were obtained using the measured data to predict how the switching voltage and holding current vary with the feedback resistance. These relationships can be used to estimate the trigger current needed for switching the SCS. The RC time constant was optimized to achieve lower dead time, which gave a higher pulse rate compared to the previous pulse mode detectors.

It was very important to note that the initial premise of building an SCS-based detection system to detect CS-137 sources was achieved. In the process of achieving this goal we not only refined the process to control the SCS and circuit I-V characteristics, but further understood the interactions of the radiation with the PD. Of particular note, the CS-137 source emits beta particles and gamma rays, whereas the AM-241 emitted only alpha particles. The observe pulses from this source is most likely due to beta radiation since they have a higher interaction cross section compared to gamma radiation.

B. RECOMMENDATIONS

Further understanding factors of efficiency should be the next focus area. It would be of great assistance if a specific application be stated and studied for the factors of efficiency in pulse generation. Having the equipment to place a known radiation source on the sensing element, as well as the ability to design and fully understand the interaction of incident radiation with the sensing element in conjunction with the produced pulse counts would accomplish this.

For ionizing radiation SCS Base Detectors specifically, thesis research should be conducted in conjunction with other laboratories that can preciously control stronger radiation sources such as Lawrence Livermore laboratories, or University of California, Berkley. Additionally, a thorough selection for photodiodes with thicker depletion region, or a photodetector made of high atomics weight materials such as CZT should more readily interact specially with the gamma radiation.

Additionally, any high gate current producing sensors such as photodiode with integrated scintillators can be employed with the SCS.

C. FEASIBILITY OF FUTURE NAVAL APPLICATIONS AND POSSIBLE FUTURE STUDIES

Use of the semiconductor-based circuits such as the one studied in this thesis can be very attractive for naval applications. Current radiation detection devices are bulky, complex and very expensive. Further study of the design of the SCS P-N-P-N layers could yield better understanding of low power SCS operation and improvement of detection sensitivities.

It is recommended that for a follow on thesis, that the feasibility of modifying this circuit to perform underwater Light Detection And Ranging (LiDAR) as an alternative for High Frequency Active (HFA) SOund Navigation And Ranging (SONAR) be explored. Ice-keel avoidance is of a key concern for submarines operating in the arctic environment. LiDAR application of less than 100m in distance would be of great use for operations in arctic passages and littoral regions. Due to the inherent properties of water,

it is well know that blue, green and Ultra-Violet (UV) wavelengths propagate to about 200 m of depth.

Modification only of the sensing element coupled with the addition of an emitter that operates in the desired spectrum is a real possibility. The sensing element can be replaced with the appropriate photodetector to sense blue, green or UV. Tuning the circuit to these wavelengths allows for the best propagation through the ocean medium. Furthermore, lasers have already been developed in these spectrums for underwater use. Study of the pulse characteristics from the returned signal can be used to correlate a known distance to a given object.

Due to very strong acoustic propagation properties in the Arctic Region, the proof of concept will provide an un-paralleled tactical advantage. Applied with further reach for un-manned senor applications, great strategic advantages can be obtained and should be strongly perused in-lieu of the future limitations of fewer fast attack submarines, and icebreaking capable ships. Development and employment of this technology should be strongly considered to counter the much greater numerical superiority and aggressive non-U.S. forces in the arctic region.

THIS PAGE INTENTIONALLY LEFT BLANK

APPENDIX A. SEMICONDUCTOR DETECTOR DESIGN CRITERION WORK SHEET

1. Given an available photodetector, proceed to the experimental determination of the photocurrent due to the radiation source to be detected (IAG).

2. From the values of photocurrent, estimate the holding current (IH) .

3. From the plot Log (IH (nA)) vs. Log (RF(ohm)), determine RF.

4. From the ratio RF:RL (1:3 for ~3V, 1:5 for ~8V switching voltages), estimate RL.

5. To optimize the speed of operation, use the lowest capacitor value (C) that allows pulsation and the Zener with the lowest breakdown voltage.

THIS PAGE INTENTIONALLY LEFT BLANK

APPENDIX B. CALIBRATION PROCEDURE

To achieve repeatable circuit responses, use best practice operating procedures where established. For initial calibration, two methods were established for circuits with either extreme sensitivity to PD stimulation and limited metered response, or less sensitive circuits with large resolution.

For sensitive circuits, the V_{BIAS} is set just prior to V_S with no I_{AG} with no pulses on the oscilloscope. After this, when the PD generates I_{AG} the SCS produces self-terminating pulses, the presence of pulses on the PD indicates that a field is present on the PD.

For circuits with poor sensitivity and large resolution, the operator applies a V_{BIAS} just past V_S with no I_{AG} to produce a steady pulse stream. After this, when the PD generates $I_{AG,}$ the display element dissipates the energy and produces additional pulses on an oscilloscope and the change in pulse frequency is indicative of a change in the induced field on the PD.

Improper calibration of V_{BIAS} by over compensating will produce pulse clipping or pulse deletion. Low V_{BIAS} will preclude the SCS from generating any pulses. Calibration was key to achieving steady, accurate and repeatable data runs.

THIS PAGE INTENTIONALLY LEFT BLANK

LIST OF REFERENCES

[1] S. Awadalla, *Solid-State Radiation Detectors Technology and Applications.* Boca Raton, FL: Taylor & Francis Group, 2015.

[2] F. Alves, C. Smith, and G. Karunasiri. (2014, September 1). A solid-state spark chamber for detection of ionizing radiation. *Sensors and Actuators A: Physical* vol. 216, pp. 102–105. Available: http://www.sciencedirect.com/science/article/pii/S0924424714002581

[3] A. D. Moore, "Optical Detection Using Four-Layer Semiconductor Structures," M.S. thesis, Dept. Applied Physics, Naval Postgraduate School., Monterey, CA, 2005.

[4] E. P. C. Casal, "Optimizing SCR design for optical detection," M.S. thesis, Dept. Applied Physics, Naval Postgraduate School., Monterey, CA, 2009.

[5] W. C. C. Chang, "Operational characteristics of a SCR-based pulse generating circuit," M.S. thesis, Dept. Applied Physics, Naval Postgraduate School, Monterey, CA, 2014.

[6] G. Karunasiri, (2006, July 10). Spontaneous pulse generation using silicon controlled rectifier. Applied Physics Letters [Online]. 89(2). pp. 23501-1–23501-3. Available: http://scitation.aip.org/content/aip/journal/apl/89/2/10.1063/1.2220528

[7] Radiation Safety Department. (n.d.). University of Cincinnati. [Online]. Available: http://researchcompliance.uc.edu/radsafety.aspx. Accessed Oct. 30, 2015.

THIS PAGE INTENTIONALLY LEFT BLANK

INITIAL DISTRIBUTION LIST

1. Defense Technical Information Center
   Ft. Belvoir, Virginia

2. Dudley Knox Library
   Naval Postgraduate School
   Monterey, California